Biomaterials 34 (2013) 7016–7032

Contents lists available at SciVerse ScienceDirect

Biomaterials

journal homepage: www.elsevier.com/locate/biomaterials

Low-modulus Mg/PCL hybrid bone substitute for osteoporotic fracture fixation

Hoi Man Wong [a], Shuilin Wu [b], Paul K. Chu [b], Shuk Han Cheng [c], Keith D.K. Luk [a], Kenneth M.C. Cheung [a], Kelvin W.K. Yeung [a,d,*]

[a] Department of Orthopaedics and Traumatology, The University of Hong Kong, Pokfulam, Hong Kong, China
[b] Department of Physics and Materials Science, City University of Hong Kong, Kowloon, Hong Kong, China
[c] Department of Biology and Chemistry, City University of Hong Kong, Kowloon, Hong Kong, China
[d] Shenzhen Key Laboratory for Innovative Technology in Orthopaedic Trauma, The University of Hong Kong Shenzhen Hospital, 1 Haiyuan 1st Road, Futian Distract, Shenzhen, China

ARTICLE INFO

Article history:
Received 31 March 2013
Accepted 24 May 2013
Available online 18 June 2013

Keywords:
Magnesium
Polycaprolactone
Biodegradable
Bioactive
Low modulus

ABSTRACT

In this paper, we describe a new biodegradable composite composed of polycaprolactone and magnesium. Incorporation of magnesium micro-particles into the polycaprolactone matrix yields mechanical properties close to those of human cancellous bone, and *in vitro* studies indicate that the silane-coated Mg/PCL composites have excellent cytocompatibility and osteoblastic differentiation properties. The bioactivity of the composites is manifested by the formation of calcium and phosphate after immersion in simulated body fluids. The bulk mechanical properties can be maintained for 2 months before obvious degradation takes place. The *in vivo* animal study reveals a larger amount of new bone formation on the silane-coated Mg/PCL composites compared to conventional PMMA and pure polycaprolactone and our results suggest potential clinical applications of the sliane-coated Mg/PCL composites.

© 2013 Elsevier Ltd. All rights reserved.

1. Introduction

Osteoporotic bone fractures afflict 200 million people worldwide, particularly women over the age of 65 [1,2] and in the United States, there are more than 1.5 million fractures annually [3]. The types of bone fractures range from vertebral fractures to extremity fractures including fractures of proximal femur, humerus, and distal radius [4]. Cement augmentation is a promising approach to repair osteoporotic fractures. Polymethylmethacrylate (PMMA) is a conventional bone cement that has been widely used in orthopedic surgery since the 1960s and it is believed to be effective in immediate bone stabilization and pain relief [5]. However, some drawbacks concerning the treatment of fragile bones have been found, for example, unsatisfactory bioactivity [6], increased risk of adjacent vertebral body fractures due to the mismatch of mechanical properties and bone [7–9], and strong exothermic reactions during polymerization which can potentially lead to adjacent soft tissue necrosis and pulmonary embolism [7,10,11]. Release of the methylmethacrylate (MMA) monomer into the vascular system has also been shown to cause sudden blood pressure drop and some fatalities have been reported [12,13]. Owing to the suboptimal properties of PMMA, fabrication of low-modulus porous PMMA bone cement had been considered [14–17]. However, this modification has not addressed adequately the issues about monomer toxicity, exothermic reaction during polymerization, and bioactivity [18]. Consequently, other types of bioactive bone cements such as calcium phosphate cements, calcium-sulfate cements, hydroxyapatite, glass ceramics, and bioactive glass have been proposed [18–21]. The advantages of calcium-based cements are that they hardened by a slow exothermic reaction which produces less heat during curing and strong integration with bone can subsequently be obtained [18]. However, the insufficient mechanical stability may hinder prolonged use [9]. To address the insufficient mechanical strength of calcium phosphate cements, different types of modification such as incorporation of high-strength beta-tricalcium phosphate aggregates and fabrication of macroporous calcium phosphate cement have been reported [22,23]. However, the improvement attained so far is still not adequate for many osteoporotic patients, particularly issues pertaining to shear and tension forces [18,22,23], and better bone substitutes are in high demand.

* Corresponding author. Department of Orthopaedics and Traumatology, The University of Hong Kong, Pokfulam, Hong Kong, China. Tel.: +852 2255 4654; fax: +852 2817 4392.
E-mail address: wkkyeung@hku.hk (K.W.K. Yeung).

0142-9612/$ – see front matter © 2013 Elsevier Ltd. All rights reserved.
http://dx.doi.org/10.1016/j.biomaterials.2013.05.062

In this paper, we describe a low-modulus bone substitute made of polycaprolactone that comprises magnesium micro-particles which alter the mechanical properties of the composites. Polycaprolactone is an FDA approved biodegradable polymer that has been widely applied to tissue engineering nowadays [24,25]. Due to its slow degradation rate and relatively low melting point, it should allow sufficient time for bone healing and easy shaping of scaffolds [26]. The literature reported that the incorporation of metallic filler into polymer matrix could alter the mechanical properties of the composites [27]. Since magnesium is a type of biodegradable metallic material and essential to bone development [28,29], this material is therefore chosen to incorporate into polycaprolactone in this study. Additionally, It has been reported that the presence of magnesium in the bone system is beneficial to bone strength and growth [30,31]. Our objectives are to determine the mechanical properties of the composites, evaluate the *in vitro* biological response including osteogenic differentiation properties as well as *in vivo* performance. The ultimate goal is to develop better materials that can minimize post-operation complications and expedite healing for patients requiring cement augmentation.

2. Materials and methods

2.1. Sample preparation

Commercial magnesium micro-particles (Mg) with 2 different sizes (i.e. 45 μm and 150 μm) (International Laboratory, USA) and polycaprolactone (PCL) (Sigma–Aldich, USA) with the average molecular weight of Mn ~ 80,000 g/mol were used. To enhance the bonding between the PCL and Mg, surface modification using the silane coupling agent of Mg was conducted. 3-(Trimethoxysilyl)propyl methacrylate (TMSPM) (Sigma, USA) was used as the silane coupling agent and the treatment parameters are shown in Table 1. The grafting quality of the silane-coated Mg micro-particles was characterized by X-ray photoelectron spectroscopy (XPS). After characterization, the silane-coated Mg micro-particles were blended homogenously with the polymer PCL in a batch mixer at 60 °C and composites with the Mg micro-particles to PCL ratio of 0.1:1 were produced. Disk samples with diameters of 5 mm, 14 mm, and 33 mm and thickness of 1 mm were prepared for the immersion tests and *in vitro* studies whereas rod samples were prepared for the mechanical tests and *in vivo* animal studies. The rod samples for the mechanical tests were 3 mm in diameter and 9 mm long and the samples used in the animal study were 2 mm in diameter and 6 mm long.

2.2. Characterization

2.2.1. Chemical analysis of the silane-coated Mg micro-particles

The surface chemical composition of the silane-coated Mg micro-particles was determined by X-ray photoelectron spectroscopy (XPS) using Al K_α irradiation. It was to ensure that the silane coupling agent was coated on the Mg micro-particles.

2.2.2. Ion leaching analysis

Immersion tests were carried out at different time points to monitor the amounts of magnesium ions released from the 45 μm and 150 μm uncoated and silane-coated Mg/PCL composites. The samples 14 mm in diameter and 1 mm thick were immersed into 10 ml of simulated body fluids (SBF) separately. The capsules containing the specimens and SBF were placed in an incubator for 7 different periods of time (6 h as well as 1, 4, 7, 14, 30 and 60 days). Five samples were analyzed at each time point by inductively-coupled plasma optical emission spectrometry (ICP-OES) (Perkin Elmer, Optima 2100DV) to determine the ion concentrations and establish the correlation between ion dissolution and time. The pH values were acquired on a pH meter and the corrosion rate was determined by measuring the weight loss from each sample. The surface and morphology of the Mg/PCL composites after the immersion test were examined by scanning electron microscopy (Leo 1530 FEG SEM) and the elemental compositions were determined by energy-dispersive X-ray spectroscopy (EDS).

2.2.3. Mechanical tests

In order to characterize the effectiveness of the TMSPM silane coating, compression tests were conducted on both the uncoated and silane-coated Mg/PCL composites. Pure PCL and PMMA served as the controls. The compression tests were performed according to the ASTM D695-08 protocol and the compressive moduli were evaluated after the compression tests. The speed was set at 1 mm/min on a materials testing system (MTS) 858.02 Mini Bionix machine.

Table 1
Treatment parameters on Mg micro-particles using TMSPM silane coupling agent.

Treatment parameters	
Mg micro-particles	45 μm or 150 μm (10 g)
Silane coupling agent	3-(Trimethoxysilyl)propyl methacrylate (TMSPM) (5 ml)
Solvent	Cyclohexane (100 ml)
Catalyst	Propylamine (2 ml)
Treatment temperature	80 °C
Treatment duration	3 h
Post heat treatment	
Temperature	80 °C
Duration	5 h
Pressure	100 mBar

2.3. In vitro studies

2.3.1. Cytocompatibility of the silane-coated Mg/PCL composites

Enhanced Green Fluorescent Protein Osteoblasts (eGFPOB) from GFP mice were cultured on the surface of the silane-coated Mg/PCL composites to determine growth and cytocompatibility. The samples were placed in a 96-well plate and 1.7×10^4 cells/cm^2 GFPOB were seeded on each sample. The cells were cultured using the Dulbecco's Modified Eagle Medium (DMEM, Invitrogen) supplemented with 10% (v/v) fetal bovine serum (Biowest, France), antibiotics (100 U/ml of penicillin and 100 μg/ml of streptomycin), and 2 mM L-glutamine. They were incubated at 37 °C in under 5% CO_2 and 95% air for 1 or 3 days afterwards. The cell morphology was observed by fluorescence microscopy (Niko ECL IPSE 80i, Japan). The attached living eGFP-expressive osteoblasts were visualized using a 450–490 nm incident filter, and the fluorescence images emitted at 510 nm were captured by a Sony DKS-ST5 digital camera.

2.3.2. Cell viability of the silane-coated Mg/PCL composites

The MTT assay was used to determine the cytotoxicity of the silane-coated Mg/PCL composites to murine cells. 7×10^4 cells/cm^2 mouse MC3T3-E1 pre-osteoblasts were cultured in the DMEM culture medium supplemented with 10% (v/v) fetal bovine serum (FBS, Biowest, France), antibiotics (100 U/ml of penicillin and 100 μg/ml of streptomycin), and 2 mM L-glutamine. They were placed on a 96-well tissue culture plate and incubated at 37 °C in an atmosphere of 5% CO_2 and 95% air for 1 day. The MTT solution was prepared by adding thiazolyl blue tetrazolium bromide powder to the phosphate buffered saline (PBS, OXOID Limited, England) and 10 μL of 5 mg/ml MTT solution was added on the first day. The well was incubated at 37 °C under 5% CO_2 and 95% air for 1 day. 100 μL of 10% sodium dodecyl sulphate (SDS, Sigma, USA) in 0.01 M hydrochloric acid was added to each well and incubated at 37 °C in an atmosphere of 5% CO_2 and 95% air overnight to form crystals. Finally, the absorbance was recorded by a mutlimode detector on the Beckman Coulter DTX 880 at a wavelength of 570 nm with a reference wavelength of 640 nm. The cell viability was determined from the absorbance readings.

2.3.3. Alkaline phosphatase (ALP) activity

The ALP assay was employed to determine the osteogenic differentiation property of the silane-coated Mg/PCL composites compared to pure PCL and PMMA. Samples measuring 14 mm in diameter and 1 mm in thickness were used. 1.4×10^4 cells/cm^2 mouse MC3T3-E1 pre-osteoblasts were cultured in the DMEM culture medium supplemented with 10% (v/v) fetal bovine serum (FBS, Biowest, France), antibiotics (100 U/ml of penicillin and 100 μg/ml of streptomycin), and 2 mM L-glutamine. The composites were placed on a 24-well tissue culture plate and incubated at 37 °C in an atmosphere of 5% CO_2 and 95% air for 1 day. On the second day, all of the culture media in each well were replaced with the differentiation DMEM medium containing 50 μg/ml ascorbic acid (Sigma, USA) and incubated at 37 °C in an atmosphere of 5% CO_2 and 95% for 3, 7 and 14 days. The culture medium was changed every 3 days and starting on day 7, 10 mM of β-glycerol phosphate (MP Biomdicals, France) was added together with ascorbic acid. After incubation, the cells were washed with PBS 3 times and lysed with 0.1% Triton X-100 at 4 °C for 30 min. The cell lysates were centrifuged at 574 g and at 4 °C for 10 min (2–5 Sartorius, Sigma, USA) and 10 ul of the supernatant of each sample was transferred to a 96-well tissue culture plate. The ALP activity was determined by a colorimetric assay using an ALP reagent containing p-nitrophenyl phosphate (p-NPP)

Table 2
Primer pairs used in real-time PCR analysis.

Gene	Forward primer	Reverse primer
Gapdh	5′-ACCCAGAAGACTGTGGATGG-3′	5′-CACATTGGGGGTAGGAACAC-3′
ALP	5′-CCAGCAGGTTTCTCTCTTGG-3′	5′-GGGATGGAGGAGAGAAGGTC-3′
Col1a1	5′-GAGCGGAGAGTACTGGATCG-3′	5′-GTTCGGGCTGATGTACCAGT-3′
Runx2	5′-CCCAGCCACCTTTACCTACA-3′	5′-TATGGAGTGCTGCTGGTCTG-3′
Opn	5′-TCTGATGAGACCGTCACTGC-3′	5′-AGGTCCTCATCTGTGGCATC-3′

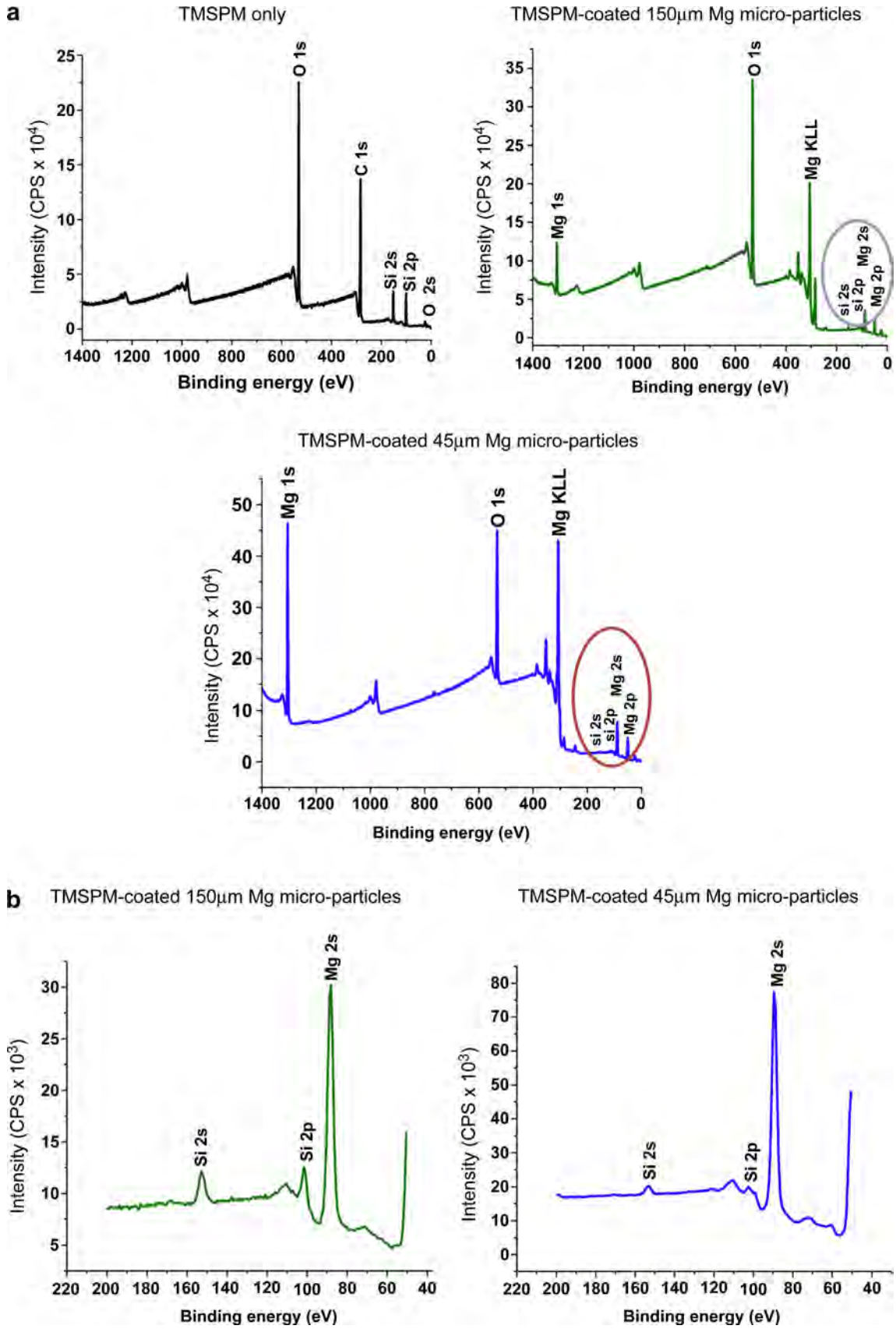

Fig. 1. (a) Survey scan of the TMSPM silane and TMSPM-coated Mg micro-particles by using X-ray photoelectron spectroscopy. The scanning range was from 0 to 1400 eV. (b) Detailed survey scan of TMSPM-coated Mg micro-particles by using X-ray photoelectron spectroscopy. The scanning range was from 50 to 200 eV. Silicon was found on the Mg micro-particles after TMSPM silane treatment.

(Stanbio, USA) as the substrate. The absorbance was recorded by the multimode detector on the Beckman Coulter DTX 880 at a wavelength of 405 nm. The ALP activity was normalized to the total protein level of the samples measured by the Bio-Rad Protein Assay (Bio-Rad, USA).

2.3.4. Real-time quantitative RT-PCR analysis

The osteogenic differentiation properties of the silane-coated Mg/PCL composites were further assessed by real-time quantitative RT-PCR to measure the relative mRNA expression levels of the commonly used bone markers including alkaline phosphatase (ALP), type I collagen (*Col1a1*), runt-related transcription factor 2 (*Runx2*) and osteopontin (*Opn*) (primer pairs used are as shown in Table 2). Samples 33 mm in diameter and 1 mm thick were used. 1.6×10^5 cells/cm^2 mouse MC3T3-E1 pre-osteoblasts were cultured in the DMEM culture medium supplemented with 10% (v/v) fetal bovine serum (FBS, Biowest, France), antibiotics (100 U/ml of penicillin and 100 μg/ml of streptomycin), and 2 mM L-glutamine. They were placed on a 6-well tissue culture plate and incubated at 37 °C in an atmosphere of 5% CO_2 and 95% air for 1 day. On the second day, the culture medium in each well were replaced by the DMEM medium containing magnesium and 50 μg/ml ascorbic acid (Sigma, USA) and incubated at 37 °C in an atmosphere of 5% CO_2 and 95% air for 3, 7 and 14 days. The culture medium was changed every 3 days and starting on day 7, 10 mM of β-glycerol phosphate (MP Biomdicals, France) was added to the DMEM medium which also contained 50 μg/ml of ascorbic acid.

After 3, 7, and 14 days, the total RNA of the osteoblasts was isolated using a TRIZOL reagent (invitrogen, USA). Chloroform was added to isolate the RNA into the aqueous phase. The upper colorless aqueous phase was transferred to a new 1.5 ml eppendorf and isopropanol was added to precipitate the RNA. Finally, the RNA pellets were washed with 75% ethanol and dissolved in RNase inhibitor diethyl pyrocarbonate (DEPC) treated water. The RNA concentrations were determined on the Nanodrop 1000 spectrophotometer (Thermo Scientific, USA). The complementary DNA (cDNA) was reverse-transcribed from 1 μg of total RNA using a high-capacity RNA-to-cDNA master mix kit (Applied Biosystem) following the manufacturer's instruction. The real-time PCR was performed on the SYBR Green PCR Master Mix (Applied Biosystems, USA). The total reaction volume was 25 μl including 12.5 μl 2× SYBR Green PCR Master Mix, 1 μl of forward and 1 μl of reverse primers, 1 μl of cDNA template, and 9.5 μl of RNase water. The reaction was carried out on the ABI prism 7900HT sequence detection system (Applied Biosystems, USA) and the standard setting with 40 cycles was used to amplify the signal. Finally, the relative mRNA expression level of each gene was normalized to the house-keeping gene glyceraldehyde-3-phosphate dehydrogenase (*Gapdh*) and determined using Ct values.

2.3.5. Magnesium ions released in the DMEM medium

In order to determine the amount of magnesium ions released from the silane-coated Mg/PCL composites during cell culturing, a short immersion test in the DMEM medium was conducted. Pure PCL and silane-coated Mg/PCL composites 14 mm in diameter and 1 mm thick were put on a 24-well plate containing 500 μl of the medium. The samples were placed in an incubator for different periods of time (i.e. 1, 2, 3, 6, 12, 24 and 48 h). Five samples were used at each time point and at each time point, the magnesium ion concentrations were determined by inductively-coupled plasma optical emission spectrometry (ICP-OES) (Perkin Elmer, Optima 2100DV). The correlation between ion dissolution and time was established.

2.3.6. Cellular response

To verify the cellular response due to Mg, the cytocompatibility and osteogenic differentiation ability for different Mg concentrations were assessed. The stock solutions were prepared by dissolving anhydrous $MgCl_2$ in deionized water and the concentrations were verified by ICP-OES (Perkin Elmer, Optima 2100DV). The solutions were diluted with Dulbecco's Modified Eagle Medium (DMEM) (Invitrogen) to final concentrations of 50, 200, 400, and 1000 ppm. The MTT assay was conducted to study the cell viability and the ALP assay and real time RT-PCR were used to evaluate the osteogenic differentiation ability of cells cultured with different concentrations of Mg. The culturing conditions were the same as those described before and the only difference was that the culture media in each well were replaced by the magnesium-supplemented DMEM after the first day.

2.4. Mechanical tests

Compression tests were conducted to determine the mechanical properties during degradation. Pure PCL and silane-coated Mg/PCL composites 3 mm in diameter and 6 mm long were immersed in 10 ml of SBF. The closed capsules containing the specimens in the solution were placed in a 37 °C incubator for different periods of time (days 1, 4, 7, 14, 30 and 60). Five samples were used for each time point. The compression test was conducted based on the ASTM D695-08 protocol to determine the mechanical properties of the Mg/PCL composites. The compressive moduli were evaluated after the compression test. The materials testing system (MTS) was the 858.02 Mini Bionix machine and the speed was 1 mm/min. The magnesium ion concentrations in the DMEM extracts were measured at each time point in order to correlate the release with the change of the compressive modulus. The magnesium ion concentrations were determined by inductively-coupled plasma optical emission spectrometry (ICP-OES) (Perkin Elmer, Optima 2100DV).

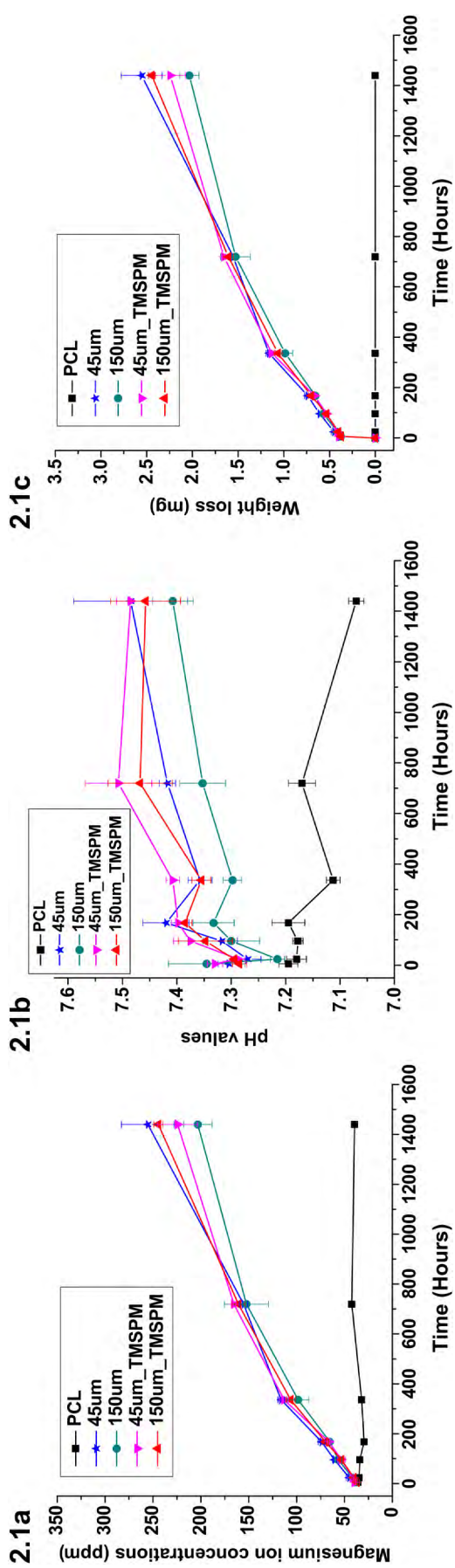

Fig. 2. (2.1a) Magnesium ions released from pure PCL, 45 μm and 150 μm uncoated and TMSPM-coated Mg/PCL composites over time. (2.1b) pH values of the immersion extract from pure PCL, 45 μm and 150 μm uncoated and TMSPM-coated Mg/PCL composites over time. Similar pattern was found on all the Mg/PCL composites. The pH values of the composites increased steadily whereas the pH value of pure PCL decreased upon 2 months degradation. (2.1c) Total weight lost from pure PCL, 45 μm and 150 μm uncoated and TMSPM-coated Mg/PCL composites over time. Similar pattern was found on all the Mg/PCL composites. (2.2a) Surface compositions of pure PCL, 45 μm and 150 μm uncoated and TMSPM-coated Mg/PCL composites after 6 h of SBF immersion using energy-dispersive X-ray spectroscopy. (2.2b) Surface compositions of 45 μm and 150 μm TMSPM-coated Mg/PCL composites after 1 day of SBF immersion using energy-dispersive X-ray spectroscopy. (2.2c) Surface compositions of pure PCL, 45 μm and 150 μm TMSPM-coated Mg/PCL composites after 2 months of SBF immersion using energy-dispersive X-ray spectroscopy.

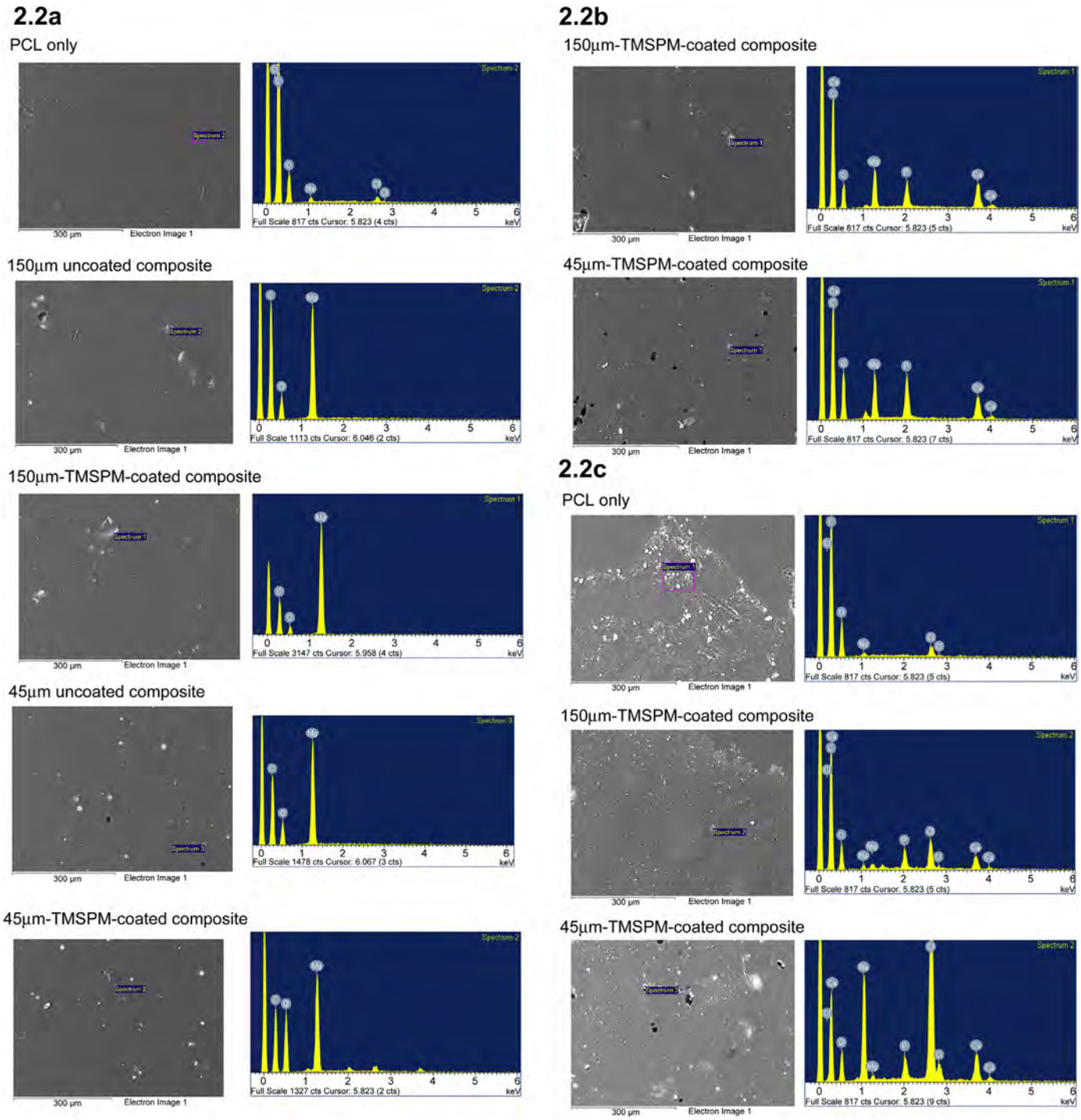

Fig. 2. (*continued*)

2.5. *In vivo animal studies*

2.5.1. *Surgical procedures*

After conducting the physical, chemical and *in vitro* biological tests, *in vivo* animal studies were performed. The anaesthetic, surgical and post-operative care protocols were examined by and fulfilled the requirements of the University Ethics Committee of The University of Hong Kong and the Licensing Office of the Department of Health of the Hong Kong Government.

Twenty 2-month old female Sprague–Dawley rats (SD rats) from the Laboratory Animal Unit of The University of Hong Kong were used. Their average weights were 200–250 g and the chosen operation site was the lateral epicondyle. Each rat was implanted with pure PCL, PMMA, or silane-coated Mg/PCL composites on either the left or right lateral epicondyle. In order to monitor new bone formation around the implants, serial time points of 1, 2, 3, 4, 8, 12, 16, 20 and 24 weeks were set. The PMMA and pure PCL served as the controls.

The rats were anaesthetised with ketamine (67 mg/kg) and xylazine (6 mg/kg) by intraperitoneal injection. The operation sites of the rats were shaved and also underwent decortication. A hole measuring 2 mm in diameter and 6 mm in depth was made by a hand driller at the lateral epicondyle using a minimally invasive approach. Subsequently, the samples were implanted into the prepared holes on either the left or right femur of the rats. The wound was then sutured layer by layer, and a proper dressing was applied over the incision. After the operation, the rats received subcutaneous injections of 1 mg/kg terramycin (antibiotics) and 0.5 mg/kg of ketoprofen. The rats were euthanized at 2 different time points (2 and 6 months of post-surgery).

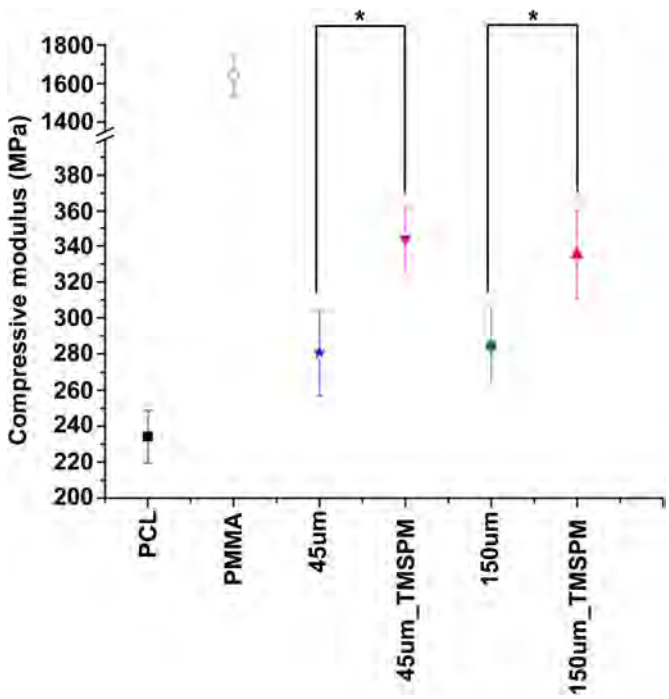

Fig. 3. Compressive moduli of pure PCL, PMMA, 45 μm and 150 μm uncoated and TMSPM-coated Mg/PCL composites prior SBF immersion. The compressive moduli of all the Mg/PCL composites were found to be significantly higher ($p < 0.05$) than pure PCL and were found to be within the range of human cancellous bone (50–800 MPa) but not PMMA. The compressive moduli of the Mg/PCL composites with silane treatment were found to be significantly higher ($p < 0.05$) as compared to the composites without silane treatment.

2.5.2. Micro-computed tomography evaluation

At each time point (i.e. 1, 2, 3, 4, 8, 12, 16, 20 and 24 weeks), micro-computed tomography (micro-CT) was conducted at the operation site to monitor the healing process and examine new bone formation around the implants. The rats were scanned in the micro-CT device (SKYSCAN 1076, Skyscan Company) at the respective time points to view new bone formation. After the 2D planes were reconstructed using the NRecon (Skyscan Company), the 3D models were generated by CTVol (Skyscan Company).

2.5.3. Fluorochrome labeling

Fluorochrome has been widely used since the 1950s [32] to determine the location of mineralization, as well as the direction and speed of bone formation with the use of different fluorochrome labels [33]. Fluorochrome labels would bind to calcium ions and take the form of hydroxyapatite crystals so as to indicate the site of new bone formation [34]. Two fluorochrome labels, xylenol orange (Sigma, USA) and calcein green (Sigma, USA) were used in this study. The fluorochrome labels were prepared according to Gaalen et al.'s study [32]. Xylenol orange was prepared by dissolving it in 2% sodium bicarbonate ($NaHCO_3$) at a concentration of 90 mg/kg. It was injected in weeks 3 and 7 post-operation. Calcein green was prepared by dissolving it in 2% $NaHCO_3$ at a concentration of 10 mg/kg and this was injected during week 5 post-operation. All the fluorochrome labels were injected into the rat subcutaneously and finally, the fluorochrome labels were viewed under a fluorescence microscopy (Niko ECL IPSE 80i, Japan) after tissue processing.

2.5.4. Magnesium ion measurements

Blood was collected prior to and at 1, 2, 3, 4, 8, 12, 16, 20 and 24 weeks post-operation to determine the magnesium ion concentration. The blood samples were centrifuged at 1339 g for 15 min at room temperature (2–5 Sartorius, Sigma, USA) and the sera were collected and stored at −20 °C. Prior to analysis, the sera were diluted 10 times in deionized water and the magnesium ion concentrations were determined by inductively-coupled plasma mass spectrometry (ICP-OES) (Optical Emission Spectrometer, Perkin Elmer, Optima 2100DV), and the concentrations of magnesium ions released from pure PCL, PMMA, and silane-coated Mg/PCL composites were compared.

The liver and kidneys of each rat were collected and stored at −20 °C after euthanization. Prior to measurement, tissue digestion was performed according to the protocol based on Ashoka et al.'s study [35]. In brief, each sample weighed approximately 0.2 g. The samples were put in a Teflon bottle and 3 ml of concentrated nitric acid and 2 ml of hydrogen peroxide were added. The Teflon bottles were placed in a hydrothermal reactor and put into an 85 °C oven for 2 h. Afterwards, the

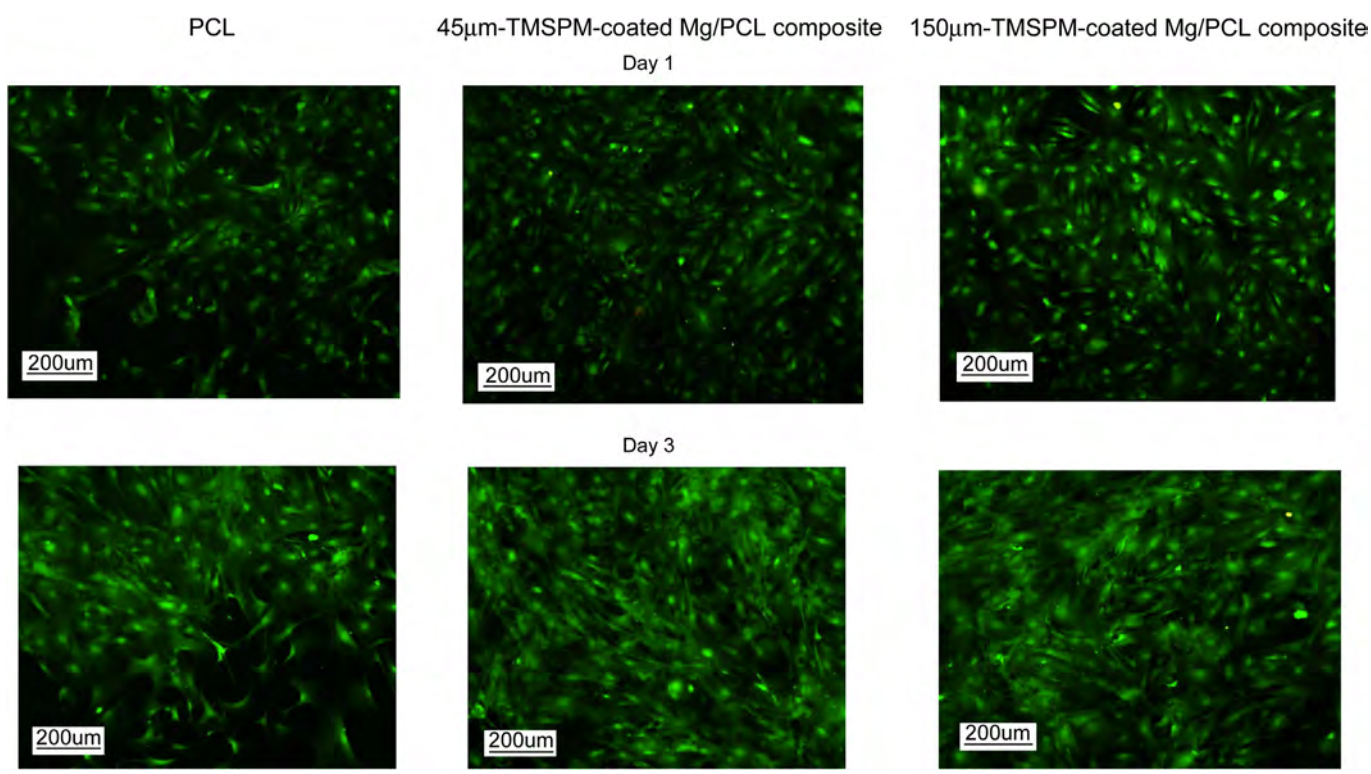

Fig. 4. Microscopic views of GFP mouse osteoblasts cultured on pure PCL, 45 μm and 150 μm uncoated and TMSPM-coated Mg/PCL composites after 1and 3 days to evaluate the cyto-compatibility of the Mg/PCL composites with and without silane treatment. 1.7×10^4 cells/cm^2 GFPOB were cultured on each sample in 96 well plate.

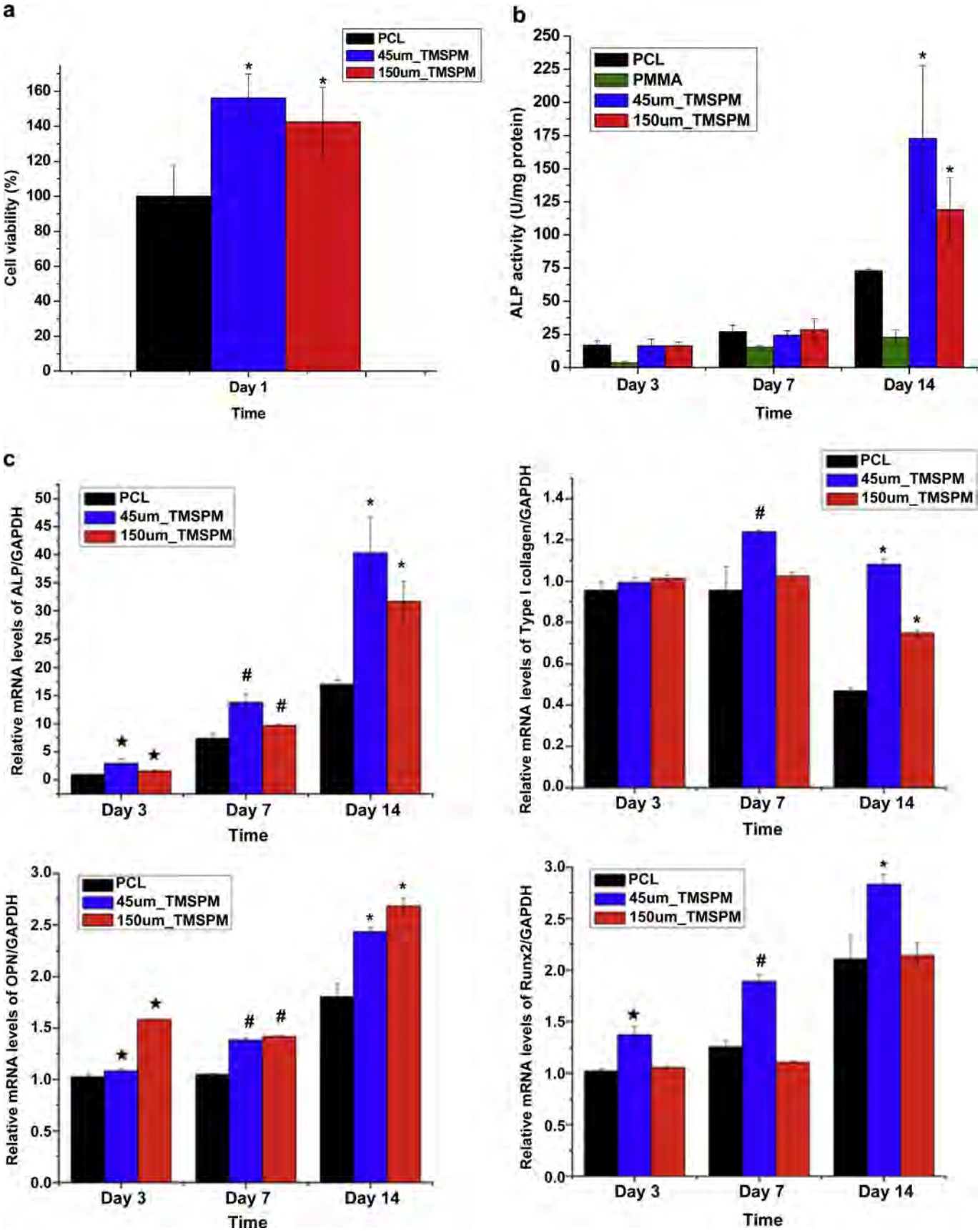

Fig. 5. (a) Cell viabilities of MC3T3-El pre-osteoblasts on pure PCL, PMMA, 45 μm and 150 μm silane-coated Mg/PCL composites using MTT assay. The readings were detected under the absorbance reading at 570 nm wavelength and the reference wavelength of 640 nm was used to determine the cell viability in comparison to the control (PCL only). Significantly higher ($p < 0.05$) cell viabilities were found on the composites as compared to pure PCL. (b) Specific ALP activities of MC3T3-El pre-osteoblasts cultured on PMMA, pure PCL, 45 μm

digested samples were diluted to 100 ml with 2% 5 M nitric acid in order to compensate for the 'acid effect' [36]. The samples were stored in a 4 °C refrigerator and the magnesium ion concentrations were determined by ICP-OES.

2.5.5. Histological analysis

The rats were euthanized 2 and 6 months post-operation and the bone samples underwent hard tissue processing. The implants were harvested and fixed in 10% buffered formalin for 3 days. A standard tissue processing step was conducted to change the samples from an aqueous stage to an organic stage. A dehydrating process was performed using 70%, 95%, and 100% ethanol, and the samples were immersed in the solutions for 3 days. Xylene was used as a transition between ethanol and methyl-methacrylate and the samples were immersed in xylene for 3 days. The methyl-methacrylate was prepared according to Erben's study [37]. The samples underwent 4 stages after xylene immersion (i.e. MMA I, MMA II, MMA III, Final stage). MMA I solution consisted of 60 ml MMA (MERCK, Germany), 35 ml of butylmethacrylate (Aldaich, USA), 5 ml of methylbenzoate (Aldaich, USA), and 1.2 ml polyethylene glycol 400 (Wako, Japan). MMA II and MMA III consisted of 100 ml MMA I with 0.4 g and 0.8 g dry benzoyl peroxide (MERCK, Germany), respectively. The MMA solutions were stirred for at least 1 h before use. The final stage consisted of treatment in 400 μl N,N-dimethyl-p-toluidine (Sigma, USA) and 100 ml cold (4 °C) MMA III. The embedded samples were then cut into sections with a thickness of 200 μm and then micro-ground down to a thickness of 50–70 μm. The sectioned samples were stained with Giemsa (MERCK, Germany) stain. The morphological and histological analyses were performed on an optical microscope to observe bone ongrowth or integration with the host tissue.

2.6. Statistical analysis

The *in vitro* experiments were conducted in triplicate and the data of the *in vitro* and *in vivo* experiments were analyzed by the one-way ANOVA and expressed as means ± standard deviations. A p value <0.05 was considered to be statistically significant.

3. Results

3.1. Characterizations

3.1.1. Surface chemical analysis

Fig. 1a shows the survey scan of the TMSPM silane coupling agent and magnesium micro-particles after the TMSPM silane treatment. As the TMSPM silane coupling agent is silicon-based, the existence of silicon suggests that the silane coupling agent has been coated on the magnesium micro-particles. As shown in Fig. 1b, silicon is detected and TMSPM has thus been successfully coated on the magnesium micro-particles.

3.1.2. Magnesium ion leaching

Fig. 2.1a presents the magnesium ion released from pure PCL, 150 μm, and 45 μm uncoated and silane-coated Mg/PCL composites. The magnesium ion concentrations leached from the 45 μm and 150 μm Mg/PCL composites are similar. The release rate increases steadily for both samples, from 39 ppm and 38 ppm after 6 h of immersion to 255 ppm and 203 ppm after 2 months (1440 h) of immersion, respectively. No significant difference is found from the Mg/PCL composites with and without TMSPM silane treatment in which the magnesium ion concentrations of silane-coated Mg/PCL composites of both 45 μm and 150 μm magnesium micro-particles throughout the immersion period vary from 40 ppm and 37 ppm after 6 h to 224 ppm and 244 ppm after 2 months, respectively.

The pH ranges of pure PCL, uncoated, and silane-coated Mg/PCL composites after 2 months of immersion are shown in Fig. 2.1b. The pH values increase from 7.2 to 7.5 for both the 45 μm and 150 μm uncoated and silane-coated Mg/PCL composites upon degradation. However, the pH value of pure PCL is found to drop below 7.1 at the 2-month time point. The weight loss shown in Fig. 2.1c corresponds to the magnesium ions released from the composites. It is found to be approximately 2.5 mg after 2 months of immersion for all the composites.

The morphology of the composites after 6 h, 1 day, and 2 months is examined by SEM and the elemental compositions are determined by EDS. Fig. 2.2a shows the morphology of the composites after 6 h of SBF immersion. The white spots on the Mg/PCL composites are magnesium micro-particles as confirmed by EDS. After immersion for 6 h, only magnesium (Mg), carbon (C), and oxygen (O) are found from the surface of all the composites and C and O are components of the polymer. After 1 day, a detectable amount of calcium and phosphate is found (Fig. 2.2b) and they can still be detected after immersion for 2 months, as shown in Fig. 2.2c. Sodium chloride (NaCl) deposition is detected from some of the composites and this impurity stems from the SBF.

3.1.3. Compression test

Fig. 3 shows the compressive moduli of pure PCL, PMMA, uncoated, and silane-coated Mg/PCL composites. The compressive moduli of the uncoated and silane-coated Mg/PCL composites are significantly higher than those of pure PCL. However, after the silane treatment, the compressive moduli of the composites are approximately 20% higher than those of the composites without silane treatment. The compressive moduli of the composites are at least 3 times smaller than those of PMMA which is within the range of human cancellous bone (50–800 MPa) [38].

3.2. In vitro studies

3.2.1. Cytocompatibility

Fig. 4 shows the viable cells on the composites after culturing for 1 and 3 days. On day 1, cell spreading is observed from the pure PCL and all the composites. After 3 days, the cells exhibit good spreading and almost grow to 100% confluence on all the silane-coated Mg/PCL composites.

3.2.2. Cell viability

Fig. 5a shows the MC3T3-E1 pre-osteoblast viability on the pure PCL and silane-coated Mg/PCL composites. Significant higher ($p < 0.05$) cell viabilities are found from the silane-coated composites compared to pure PCL. The cell viabilities on the silane-coated Mg/PCL composites are at least 40% higher than those on pure PCL.

3.2.3. ALP activities

Fig. 5b shows the specific ALP activities of PMMA, pure PCL, and silane-coated PCL/Mg composites after 3, 7 and 14 days of MC3T3-E1 pre-osteoblasts culturing. Significantly lower ALP activities are found from the PMMA throughout the experimental period compared to pure PCL and all the composites. No significant difference is found on the 45 μm and 150 μm silane-coated Mg/PCL composites on both day 3 and day 7. However, the specific ALP activities of the composites on day 14 are significant higher

and 150 μm TMSPM-coated Mg/PCL composites on day 3, day 7 and day 14. The readings were detected under the absorbance reading at 405 nm wavelength. Significantly lower ($p < 0.05$) specific ALP activity was found on PMMA during the whole experimental period as compared to other groups. Additionally, significantly higher ($p < 0.05$) specific ALP activity was found on the silane-coated Mg/PCL composites on day 14 as compared to pure PCL. (c) Osteogenic differentiation properties, which were assessed by measuring the mRNA expression level of alkaline phosphatase (ALP), type I collagen (*Col1a1*), osteopontin (*Opn*) and runt-related transcription factor 2 (Runx2) on days 3, 7 and 14. The mRNA level was normalized with the house keeping gene Glyceraldehyde 3-phosphate dehydrogenase (Gapdh). Significantly higher ($p < 0.05$) expression levels of ALP and Opn of the cells cultured on 45 μm and 150 μm composites on days 3, 7 and 14 as compared to pure PCL (Control), whereas significantly higher ($p < 0.05$) expression level of *Col1a1* was found on days 7 and 14 of 45 μm composites and day 14 on 150 μm composites. Lastly, significantly higher ($p < 0.05$) expression level of Runx2 was found on days 3, 7 and 14 of 45 μm composites.

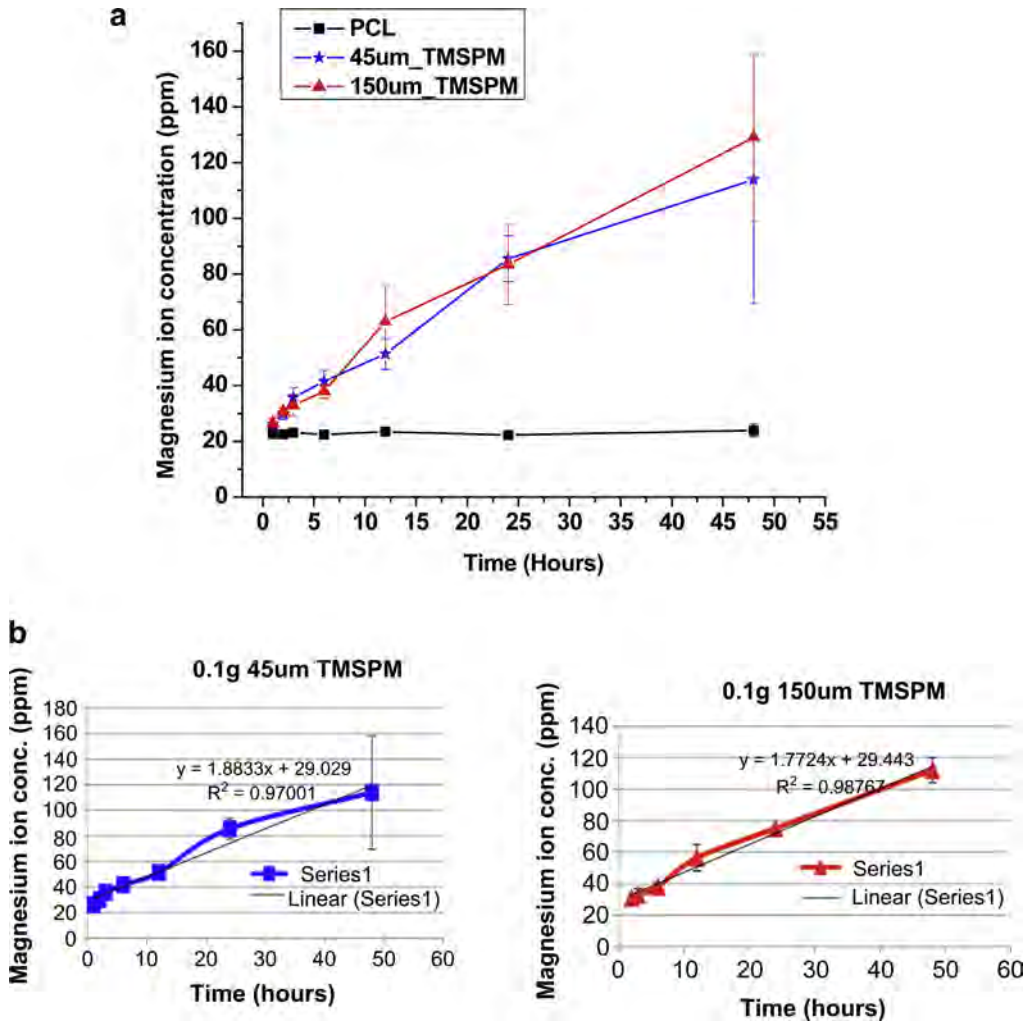

Fig. 6. (a) Magnesium ions released from pure PCL, 45 μm and 150 μm TMSPM-coated Mg/PCL composites in DMEM medium over time. (b) Magnesium ions release rate of 45 μm and 150 μm TMSPM-coated Mg/PCL composites in DMEM over time. The release rates of the composites were found to be linear.

($p < 0.05$) than those on pure PCL. The values of the 45 μm and 150 μm silane-coated Mg/PCL composites are 100 U/mg protein and 47 U/mg protein higher than those of pure PCL.

3.2.4. Real-time RT-PCR

After checking the osteoblastic differentiation properties by the ALP assay, the properties are further assessed by real-time RT-PCR. Fig. 5c shows the ALP, *Col1a1*, *Runx2* and *Opn* mRNA levels of MC3T3-E1 pre-osteoblasts cultured on pure PCL and silane-coated PCL/Mg composites. The ALP and *Runx2* mRNA levels of all the samples increase gradually with culturing time. Significantly higher ($p < 0.05$) ALP and *Opn* expressions are found from both the 45 μm and 150 μm silane-coated Mg/PCL composites on days 3, 7, and 14 compared to pure PCL. Moreover, the 45 μm silane-coated Mg/PCL composites show a significantly higher *Runx2* expression on days 3, 7, and 14 than pure PCL. The 150 μm silane-coated Mg/PCL composites show a significantly higher *Col1a1* expression on day 14 whereas the 45 μm silane-coated Mg/PCL composites exhibit a significantly higher *Col1a1* expression on both days 7 and 14 than pure PCL. The data show that the new silane-coated composites are favorable for osteoblastic differentiation.

3.2.5. Magnesium ions concentrations in DMEM

Fig. 6a shows the amount of magnesium ions released from the pure PCL and silane-coated Mg/PCL composites to the DMEM after immersion for 1 to 48 h. The release rates are calculated from the slope of the magnesium ion concentration curves in Fig. 6b. A similar release pattern is found from the silane-coated Mg/PCL composites with two different particle sizes. The release rates from the 45 μm and 150 μm silane-coated Mg/PCL composites are between 1.8 and 1.9 ppm/hour and the release rate is nearly linear with time. Table 3 shows the magnesium ion concentrations at particular time points. The values highlighted in bold are the predicted magnesium ion concentrations at 72 h based on the calculated release rate until 48 h. The magnesium ion concentrations released from the 45 μm and 150 μm silane-

Table 3
Values of magnesium ion concentrations of TMSPM-coated Mg/PCL composites after 1 h to 72 h DMEM immersion. The values highlighted in bold were the predicted magnesium ion concentrations on 72 h.

Hour	45 μm TMSPM (ppm)	150 μm TMSPM (ppm)
1	26.05	26.58
2	29.98	30.77
3	35.65	32.83
6	41.63	37.98
12	51.33	56.36
24	85.51	75.15
48	113.86	112.00
72	**164.50**	**157.00**

coated Mg/PCL composites are predicted to be 164.5 and 157 ppm, respectively.

3.2.6. Cellular response to Mg ions

Fig. 7a shows the MC3T3-E1 pre-osteoblast cell viability in the magnesium supplemented DMEM media. The cell viability after culturing in DMEM containing 50 ppm magnesium is significantly higher ($p < 0.05$) than that of the control, whereas for 200 ppm magnesium, the cell viability drops to approximately 86%. When the Mg concentration in the medium is increased, lower cell viability is observed (50% reduction at 1000 ppm Mg). Fig. 7b shows the specific ALP activities of the MC3T3-E1 pre-osteoblasts cultured in the media supplemented with magnesium after culturing for 3, 7, or 14 days. On days 3 and 14, no significant differences are found between the control, 50 ppm, and 200 ppm Mg. The highest activity is found on day 7 when there is a significantly higher specific ALP activity ($p < 0.05$) for the cells cultured in the media containing 50 ppm magnesium (147.6 U/mg protein) compared to the control (113.4 U/mg protein). The osteogenic differentiation properties are further assessed by real-time RT-PCR of ALP, *Col1a1*, *Runx2* and *Opn* mRNA expression (as shown in Fig. 7c). All the gene expressions cultured with different concentrations of magnesium ions increase gradually with culturing time. Significantly higher *Col1a1* and *Opn* expressions are found from the cells cultured with 50 ppm of magnesium than the control and sample with 200 ppm Mg on day 3. The expressions of ALP and *Runx2* of 50 ppm magnesium ion concentration are significantly higher on day 7 but not on day 3 compared to the control and 200 ppm sample.

3.3. Mechanical tests during degradation

Fig. 8a shows the compressive moduli of the samples after immersing in SBF for 60 days and no significant change of the compressive moduli can be found from the pure PCL, 45 μm, and 150 μm silane-coated Mg/PCL composites throughout the immersion period. The compressive moduli of pure PCL range from 248.6 MPa before immersion to 288.7 MPa after 2 months, whereas the compressive moduli of 45 μm and 150 μm silane-coated Mg/PCL composites range from 331.5 MPa to 356.3 MPa and 343.9 MPa to 350.7 MPa, respectively. The corresponding magnesium ion concentrations in the immersion extracts are shown in Fig. 8b to correlate with the compressive moduli. The magnesium ion concentrations of the silane-coated composites are in the range between 36 ppm and 45 ppm and a steady release rate is found throughout the immersion period.

3.4. In vivo animal study

3.4.1. Micro-computed tomography analysis

New bone formation after operation is monitored at particular time points by micro-computed tomography. Fig. 9a and b shows the cross sections of the femur with the implant after surgery and the 3D models of the newly formed bone around the implant at 2 and 6 months, respectively. The newly formed bone is indicated by red arrows and the implant is indicated by yellow arrows. The percentage changes in the bone volume are shown in Fig. 9c. Increased bone volume is found from the PMMA, PCL, 45 μm, and 150 μm silane-coated Mg/PCL composites throughout the implantation period. Significantly more new bone formation is found from the new composites from weeks 1 to 4 compared to pure PCL and also PMMA. More than 15% new bone formation is found from the Mg/PCL composites 1 week after operation and approximately 40% more new bone is found after 3 weeks compared to pure PCL. Furthermore, more than 20% new bone is found from the new composites 1 month after operation compared to PMMA.

3.4.2. Magnesium ion concentration measurement

Fig. 10a shows the percentage changes in the serum magnesium concentrations of the PMMA, PCL, 45 μm, and 150 μm silane-coated Mg/PCL composites before surgery and up to 24 weeks (6 months) post-operation. The serum magnesium concentrations of the rats implanted with different samples fluctuate from −40% to 90% and no significant difference can be found between pre-operation and throughout implantation period of all the samples.

Fig. 10b and c shows the kidney and liver magnesium ion levels, respectively, after implantation for 2 and 6 months and no significant difference can be found. The kidney magnesium ion concentrations after implantation for 2 months are in the range of 2.0–2.7 ppm/g and 1.6–2.2 ppm/g after 6 months. In addition, the magnesium ion concentrations in the liver after 2 and 6 months range from 2.1 to 2.5 ppm/g and 1.8–3.0 ppm/g, respectively.

3.4.3. Histological evaluation

Fig. 11a shows the fluorochrome labeling and histological analysis of the new bone tissue formed around the implants 2 months after implantation. Fig. 11a(i) shows the photographs with fluorochrome labels in which they could be used to compare with the Giemsa stained histological photographs in Fig. 11a(ii) at the same magnification. Both fluorochrome labels and Giemsa staining locate new bone formation around the implants. Xylenol orange gives a red color while calcine green gives a green color under fluorescence microscopy in fluorochrome labeling and Giemsa staining yields a purple color under optical microscopy. In addition, no giant cells or macrophages are found. Fig. 11b shows the histological analysis of the bone around the implants 6 months after implantation. Compared to the photographs taken after 2 months, more new bone tissues are formed around the implants. The black dots at the implant site are magnesium micro-particles.

4. Discussion

An ideal augmentation material should have certain properties including suitable injectability, ease of handling, suitable adapted viscosity, low curing temperature, adapted and lasting mechanical properties, biocompatibility, bioactivity, and slow degradation [20]. Studies have reported that cements with mechanical properties similar to cancellous bone may be beneficial in terms of reducing the fracture risks, and also reinforcing the non-fracture osteoporotic bone without altering the stress distribution significantly under physiological loading [14,15]. Hence both PMMA and calcium-based bone cements may not be the best choice due to their mismatch mechanical properties with human bone.

In this study, we fabricate a composite by incorporating magnesium micro-particles into polycaprolactone matrix with adjustable mechanical properties. Magnesium ions are essential to human metabolism and naturally found in bone tissues. Zreiqat et al. [39] have reported that the presence of magnesium ions means that it is possible to enhance osteoblast adhesion on alumina. Li et al. [40] have shown that magnesium is one of the most important bivalent ions associated with the formation of biological apatite and has no inhibitory effects on the growth of marrow cells. Both Rude et al. [41,42] and Toba et al. [43] suggest that magnesium supplementation affects bone metabolism, while magnesium deficiency results in impaired bone growth and increased bone resorption in trabecular bone. Hence, magnesium ions play an important role in many biological functions such as bone metabolism.

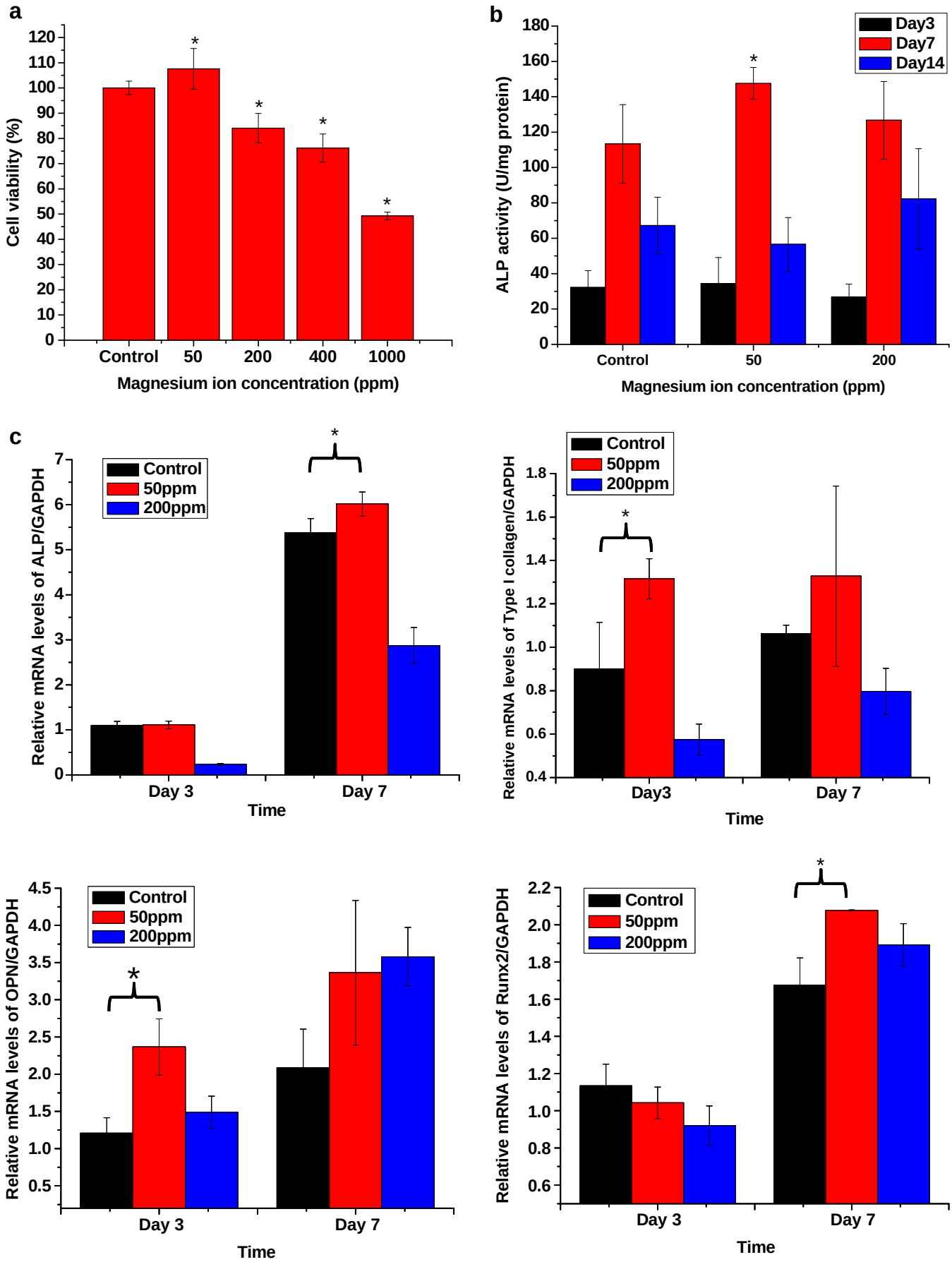
a
Cell viability (%)
Control
50
200
400
1000
Magnesium ion concentration (ppm)
b
ALP activity (U/mg protein)
Day3
Day7
Day14
Control
50
200
Magnesium ion concentration (ppm)
c
Relative mRNA levels of ALP/GAPDH
Control
50ppm
200ppm
Day 3
Day 7
Time
Relative mRNA levels of Type I collagen/GAPDH
Control
50ppm
200ppm
Day3
Day 7
Time
Relative mRNA levels of OPN/GAPDH
Control
50ppm
200ppm
Day 3
Day 7
Time
Relative mRNA levels of Runx2/GAPDH
Control
50ppm
200ppm
Day 3
Day 7
Time

The silane coupling agent [44,45] is one of the most commonly used materials to modify inorganic particles to improve the adhesion between the inorganic particles and polymer matrix [46,47]. With the use of the TMSPM sliane coupling agent which acts as an interface between the Mg micro-particles and PCL, the compressive modulus increases significantly compared to the uncoated Mg/PCL composites. However, according to the SBF immersion test, when compared to the magnesium ion released and weight lost of the composites with and without silane coating, no significant difference is found. Therefore, the results suggest that the TMSPM silane treatment is able to alter the mechanical properties of the composites by forming better bonding between the Mg and PCL instead of altering the magnesium ions release pattern. Moreover, magnesium hydroxide is formed during the degradation of magnesium micro-particles, which may help neutralize or even increase the pH as acidic products are formed during PCL degradation [26]. This is very important since slightly alkaline conditions may be more favorable to bone formation [48].

The immersed composites are examined by scanning electron microscopy at different time points and calcium and phosphate are detected from the magnesium micro-particles after immersion for 1 day, suggesting the formation of surface apatite [49,50]. With the apatite layer composed of magnesium, calcium, phosphate, and hydroxide formed on the composites, the osteoinductivity, osteoconductivity, and bone layer can be enhanced [51]. Therefore, the release of magnesium ions from Mg/PCL composites is able to promote bone growth. According to the results of the GFP osteoblasts culture and cell viability, cells grow very well on the silane-coated Mg/PCL composites and no toxic effects can be observed. In fact, according to the report of the biocompatibility screening of different silane coupling agents, toxic effects can only be found at high concentrations [52].

The osteogenic differentiation properties are also important since the major applications of the substitutes are bone-related. If the composites possess osteogenic differentiation properties, they can promote bone healing. According to the ALP assay, significantly lower specific ALP activity is found from the control PMMA due to its non-bioactive property [16]. In contrast, significantly higher specific ALP activities are found from the silane-coated composites after day 14 suggesting that the new composites favor osteoblastic differentiation. The result can be explained by optimal magnesium release during the cell culture. According to Fig. 7a–c, the proper amount of magnesium ions can enhance cell viability and osteoblastic differentiation. As the magnesium ion released from the composites is below 200 ppm throughout the SBF immersion period for up to 2 months and also short term DMEM immersion, the increase in magnesium ion concentrations are within 50 ppm from 24 h to 48 h. Indeed, it is expected that the concentrations should be similar from 48 h onwards according to the calculation. Therefore, this explains why the silane-coated composites are able to enhance osteogenic differentiation compared to the pure PCL. Consistent results are obtained from the qRT-PCR studies and significantly higher ALP expression is found from the silane-coated Mg/PCL composites. The results are further validated by Hussain et al.'s study [53], who has reported that by adding magnesium calcium phosphate into gelatin sponges, a higher level of ALP activity can be obtained as compared to the sponges without magnesium calcium phosphate. Also, the ALP activity increases with increasing amounts of added magnesium calcium phosphate. Although Hussain et al. do not show that magnesium is directly involved in the ALP activity, they suggest that the presence of magnesium is one of the reasons for the enhanced ALP

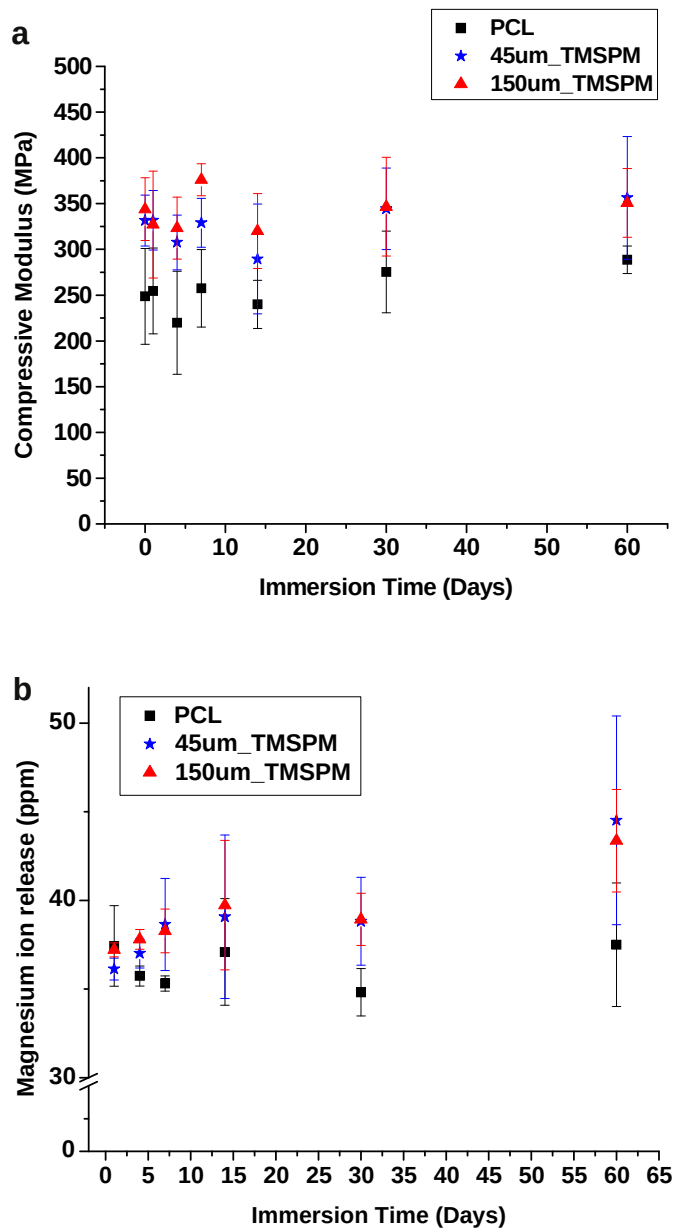

Fig. 8. (a) Compressive moduli of pure PCL, 45 μm and 150 μm TMSPM-coated Mg/PCL composites in SBF immersion up to 2 months. (b) Corresponding magnesium ion concentrations from the immersion extracts. No significant difference of the compressive moduli of pure PCL and sliane-coated composites was found.

Fig. 7. (a) Cell viabilities of MC3T3-El pre-osteoblasts cultured in medium with different concentrations of magnesium ions. The absorbance was detected at a wavelength of 570 nm with a reference wavelength of 640 nm to determine the cell viability in comparison to the control (no added magnesium ions). The percentage cell viability was calculated by dividing the absorbance values of the samples to the control. All the values were found to be significantly different ($p < 0.05$) when compared to the control. (b) Specific ALP activities of MC3T3-El pre-osteoblasts cultured in medium with different concentrations of magnesium ions on Day 3, Day 7 and Day 14. The absorbance was detected at 570 nm wavelength and the ALP activity was normalized to the total protein level of the samples. * denotes a significant difference to the control ($p < 0.05$). (c) Osteogenic differentiation was assessed by measuring the mRNA expression level of alkaline phosphatase (ALP), type I collagen (*Col1a1*), osteopontin (*Opn*) and runt-related transcription factor 2 (Runx2) after days 3 and 7. The mRNA level was normalized with the house keeping gene glyceraldehyde 3-phosphate dehydrogenase (Gapdh). Significantly higher ($p < 0.05$) expression levels of *Col1a1* and *Opn* were found with the cells cultured in 50 ppm magnesium ion concentration medium as compared to normal medium (Control), whereas significantly higher ($p < 0.05$) expression levels of ALP and Runx2 was found on day 7.

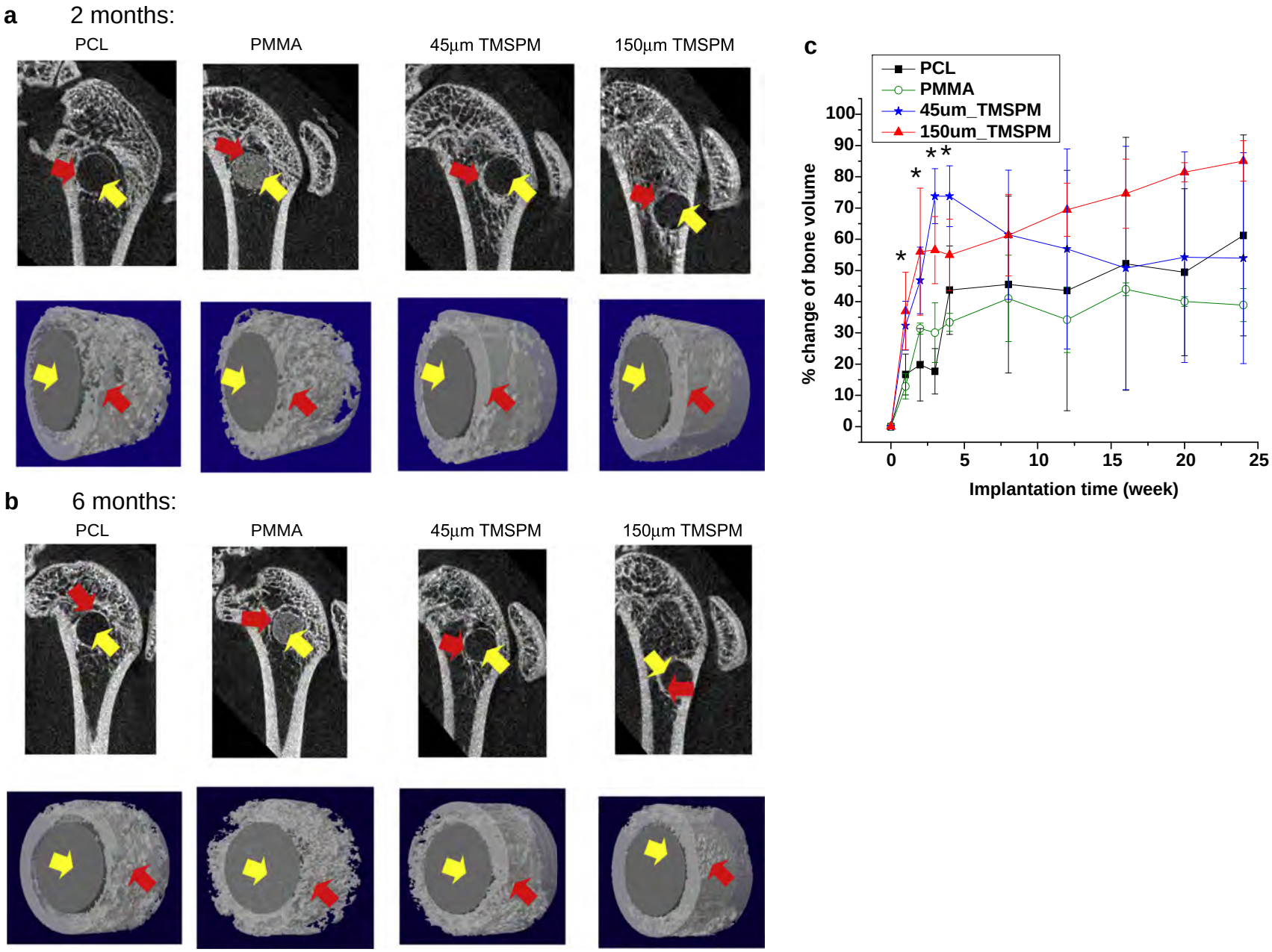

Fig. 9. Micro-CT reconstruction images of the lateral epicondyl and Micro-CT 3D reconstruction models of the newly formed bone (red arrows) around PMMA, PCL, 45 μm and 150 μm TMSPM-coated Mg/PCL composites (yellow arrows) after (a) 2 months and (b) 6 months post-operation. (c) The percentage changes in bone volume around PMMA, pure PCL, 45 μm and 150 μm TMSPM-coated Mg/PCL composites immediately after surgery and 1, 2, 3, 4, 8, 12, 16, 20 and 24 weeks of post-operation. Significantly more bone was found on the composites from week 1 to week 3 as compared to pure PCL and PMMA. (For interpretation of the references to colour in this figure legend, the reader is referred to the web version of this article.)

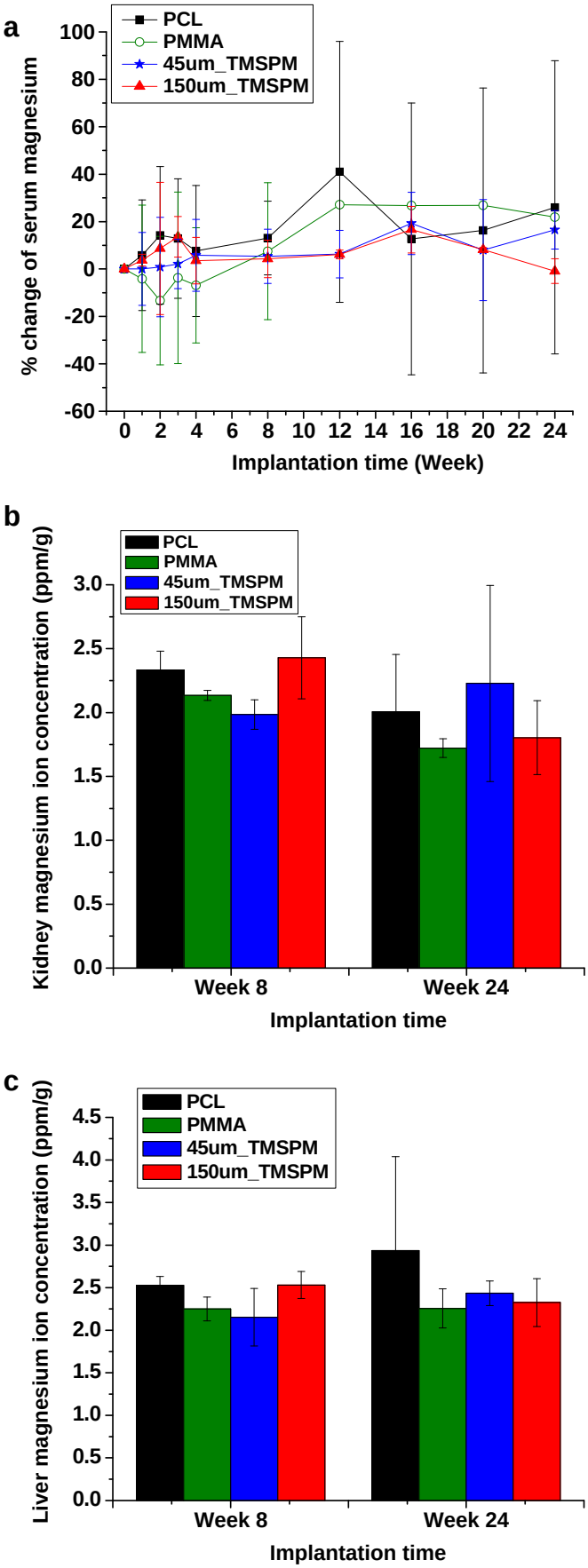

activity. Hence, magnesium has certain effects on the ALP activity. However, the mechanism of up-regulation of alkaline phosphatase activity by magnesium ions has not been well studied systematically. Moreover, the higher expressions of the other 3 bone markers on the silane-coated Mg/PCL composites illustrate the important roles in the osteogenic differentiation enhancement. The results suggest that the silane-coated Mg/PCL composites are able to enhance the differentiation and bone formation.

Before conducting the *in vivo* animal studies, the mechanical properties are first evaluated. The mechanical properties during degradation are critical to orthopedic applications because they must be maintained during degradation until bone healing. After immersion for 2 months, no significant difference is found from the silane-coated Mg/PCL composites by comparing the compressive moduli before immersion, suggesting that the suitability of the materials as orthopedic implants.

Bone formation is quantified by micro-computed tomography. More bone formation is observed from the silane-coated Mg/PCL composites than PMMA and PCL, especially at the early time points before 1 month, showing that the composites are able to enhance bone formation in a shorter period of time after implantation. Bone formation is mainly attributed to magnesium. The silane-coated Mg/PCL composites are reported to have significantly higher specific ALP activities and up-regulation of the bone-related markers than pure PCL. This explains why the silane-coated Mg/PCL composites attract more new bone formation and better osteoconductivity than PMMA and PCL at the early time points. Moreover, owing to the slow release from the composites during degradation, no gas bubbles are found around all the composites during the implantation period [54,55]. Although a similar bone volume is found compared to PMMA and PCL after 6 months of implantation, the Mg composites are able to stimulate new bone formation in a shorter period of time and so the overall healing time is shortened.

Fluorochrome labeling is used to locate the site of new bone formation since it is designed to bind with calcium ions and be incorporated into the site of mineralization [32]. Therefore, by using different fluorochrome labels at different injection times, new bone formed at different periods can be located. The results of the fluorochrome labeling can also be used to correlate with the histological photographs with Giemsa staining. Since xylenol orange and calcine green are injected on weeks 3, 5 and 7, new bone can be formed continuously on the silane-coated Mg/PCL composites. No apparent inflammation or adverse effects are found around from the implants indicating good biocompatibility.

During degradation of the silane-coated Mg/PCL composites, magnesium ions are released. They are absorbed by the body, circulate through blood and body fluid, and are stored in bone, muscle, serum and different types of cells. The excess amount of magnesium ions not absorbed by the body is excreted in the urine and since the kidneys regulate the excretion of magnesium, side-effects caused by excess amounts of magnesium ions in body are rare [56]. However, in order to make sure that the new composites are safe to use, the magnesium ion concentrations in the serum, kidney, and liver are checked. According to the magnesium ion concentration in the serum, no significant difference is found before and after implantation, indicating that degradation of magnesium

Fig. 10. (a) Percentage changes in serum magnesium levels before and after implantation. Whole blood was separated by centrifugation and the serum isolated and collected for analysis of serum Mg levels. Magnesium ion levels in (b) kidney, (c) liver after 8 weeks (2 months) and 24 weeks (6 months) implantation. The magnesium ion concentration was determined by inductively-coupled plasma optical emission spectrometry (ICP-OES). No significant difference was found with different samples at different time points.

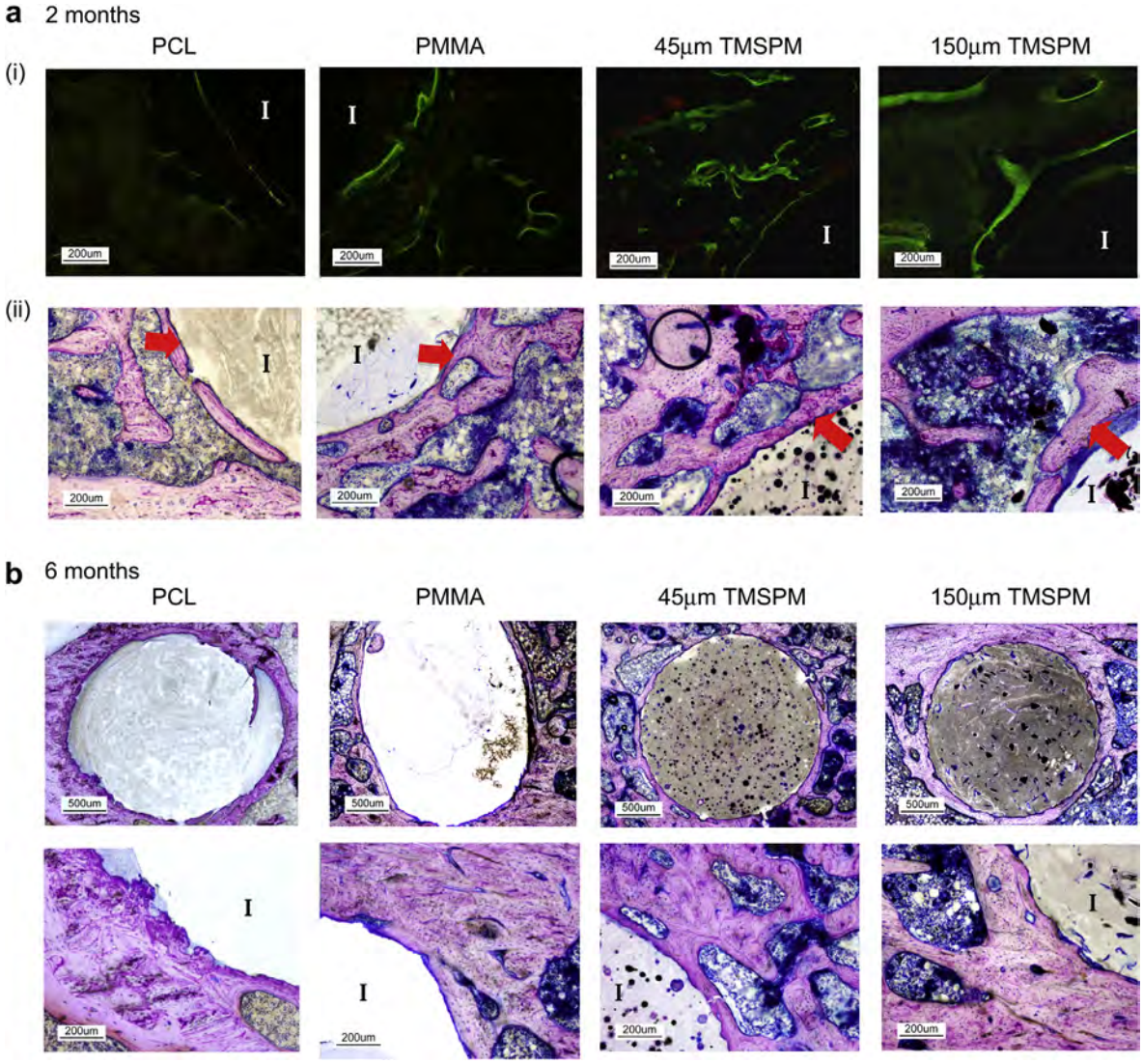

Fig. 11. (a) (i) Fluorochrome labeling and (ii) histological photographs of Giemsa stained bone tissue formed around the implants after 2 months' implantation in the lateral epicondyl. 'I' represented the implant location and red arrows show the location of newly formed bone after Giemsa staining. (b) Histological photographs of Gimesa stained bone tissue formed around the implants after 6 months' implantation in the lateral epicondyl. Photographs on the upper row are the low magnification (40×) pictures showing the whole structure of bone around the implants, whereas photographs on the lower row are pictures with higher magnification (100×) showing the new bone formation around the implants. 'I' represented the implant location. (For interpretation of the references to colour in this figure legend, the reader is referred to the web version of this article.)

does not increase the magnesium ion concentration in the serum. All the serum magnesium levels are under the recommended one and therefore safe [57]. Furthermore, no significant difference is found from the Mg concentrations in the kidney and liver, providing evidence that the magnesium ions do not produce deleterious effects.

Based on the *in vitro* and *in vivo* studies, with the addition of magnesium micro-particles, bone substitutes with adequate biodegradability, biocompatibility, osteoconductivity, and suitable mechanical properties can be fabricated. More importantly, the silane-coated Mg/PCL composites stimulate new bone formation especially at the early time points and so the healing time can be shortened. The newly developed materials have potential orthopedic applications, especially osteoporotic bone augmentation for either filling bone defects or percutaneous vertebroplasty to treat vertebral compression fracture. Although the most commonly used bone cement for vertebroplasty nowadays is PMMA, it has been reported that the mismatch in mechanical properties between PMMA and human cancellous bone can significantly increase the risk of adjacent vertebral body fractures [8,58,59]. Therefore, the new composites may solve the problems. Additionally, this study demonstrates the idea of controlling the mechanical properties of the composites by incorporating magnesium micro-particles. With different concentrations of magnesium micro-particles incorporated, composites with tailored mechanical strength can in principle be produced.

5. Conclusion

This study demonstrates the feasibility of the silane-coated Mg/PCL composites as bone substitutes in bone augmentation. By incorporating magnesium micro-particles, the compressive moduli of the composites can be adjusted to be within the range of human cancellous bone. Cells grow and proliferate well on the silane-treated Mg/PCL composites supplying evidence of good cytocompatibility. Moreover, the silane-coated Mg/PCL composites show beneficial effects on osteoblastic differentiation suggesting

that the composites can stimulate new bone formation. Furthermore, the compressive moduli of the silane-coated composites are maintained after 2 months of SBF immersion revealing that they are able to provide sufficient mechanical support prior to completely bone healing. Finally, the *in vivo* animal studies show no inflammation and more new bone formation on the silane-coated Mg/PCL composites compared to the PCL and currently used bone substitute PMMA. Hence, this bone substitute with good degradability, biocompatibility, osteogenic differentiation properties, and mechanical properties have potential clinical applications.

Acknowledgements

This study was financially supported by the AO Trauma Research Grant 2012, Hong Kong Research Grant Council General Research Funds (GRF) #718507 and #112211, City University of Hong Kong Applied Research Grants #9667066, Shenzhen Key Laboratory for Innovative Technology in Orthopaedic Trauma, The University of Hong Kong Shenzhen Hospital and HKU University Research Council Seeding Fund.

Appendix A. Supplementary data

Supplementary data related to this article can be found at http://dx.doi.org/10.1016/j.biomaterials.2013.05.062.

References

[1] Barrette-Connor E. The economic and human costs of osteoporotic fracture. Am J Med 1995;98:3S–8S.
[2] Iqbal MM. Osteoporosis: epidemiology, diagnosis, and treatment. South Med J 2000;93:2–18.
[3] Cornell CN. Internal fracture fixation in patients with osteoporosis. J Am Acad Orthop Surg 2003;11(2):109–19.
[4] Dennison E, Cooper C. Epidemiology of osteoporotic fractures. Horm Res 2000;54:58–63.
[5] Charnley J. Anchorage of the femoral head prosthesis to the shaft of the femur. J Bone Joint Surg Am 1960;42B:28–30.
[6] Hernandez L, Gurruchaga M, Goni I. Injectable acrylic bone cements for vertebroplasty based on a radiopaque hydroxyapatite. Formulation and rheological behaviour. J Mater Sci Mater Med 2008;20:89–97.
[7] Belkoff SM, Molloy S. Temperature measurement during polymerization of polymethylmethacrylate cement used for vertebroplasty. Spine 2003;28(14):1555–9.
[8] Grados F, Depriester C, Cayrolle G, Hardy N, Deramond H, Fardellone P. Long-term observations of vertebral osteoporotic fractures treated by percutaneous vertebroplasty. Rheumatology 2000;39(12):1410–4.
[9] Piazzolla A, De Giorgi G, Solarino G. Vertebral body recollapse without trauma after kyphoplasty with calcium phosphate cement. Musculoskelet Surg 2011;95:141–5.
[10] Larsson S. Cement augmentation in fracture treatment. Scand J Surg 2006;95:111–8.
[11] Ahn DK, Choi DJ, Lee S. Spinal cord injury caused by bone cement after percutaneous vertebroplasty: one case of long-term follow-up and the result of delayed removal. J Korean Orthop Assoc 2009;44:386–90.
[12] Bai B, Jazrawi LM, Kummer FJ, Spivak JM. The use of an injectable, biodegradable calcium phosphate bone substitute for the prophylactic augmentation of osteoporotic vertebrae and the management of vertebral compression fractures. Spine 1999;24(15):1521–6.
[13] Lim TH, Brebach GT, Renner SM, Kim WJ, Kim JG, Lee RE, et al. Biomechanical evaluation of an injectable calcium phosphate cement for vertebroplasty. Spine 2002;27(12):1297–302.
[14] Boger A, Heini P, Windolf M, Schneider E. Adjacent vertebral failure after vertebroplasty: a biomedical study of low-modulus PMMA cement. Eur Spine J 2007;16:2118–25.
[15] Boger A, Bohner M, Heini P, Schwieger K, Schneider E. Performance of vertebral cancellous bone augmented with compliant PMMA under dynamic loads. Acta Biomater 2008;4:1688–93.
[16] Arens D, Rothstock S, Windolf M, Boger A. Bone marrow modified acrylic bone cement for augmentation of osteoporotic cancellous bone. J Mech Behav Biomed Mater 2011;4(8):2081–9.
[17] Lopez-Heredia MA, Sa Y, Salmon P, de Wijn JR, Wolke JGC, Jansen JA. Bulk properties and bioactivity assessment of porous polymethylmethacrylate cement loaded with calcium phosphates under simulated physiological conditions. Acta Biomater 2012;8(8):3120–7.
[18] Larsson S, Bauer TW. Use of injectable calcium phosphate cement for fracture fixation: a review. Clin Orthop Relat Res 2002;395:23–32.
[19] Castaldini A, Cavallini A. Setting properties of bone cement with added synthetic hydroxyapatite. Biomaterials 1985;6(1):55–60.
[20] Heini PF, Berlemann U. Bone substitutes in vertebroplasty. Eur Spine J 2001;10:S205–13.
[21] Wang YB, Xie XH, Li HF, Wang XL, Zhao MZ, Zhang EW, et al. Biodegradable CaMgZn bulk metallic glass for potential skeletal application. Acta Biomater 2011;7(8):3196–208.
[22] Xue ZL, Zhang H, Jin AM, Ye JD, Ren L, Ao J, et al. Correlation between degradation and compressive strength of an injectable macroporous calcium phosphate cement. J Alloys Compd 2012;520:220–5.
[23] Gu T, Shi HS, Ye JD. Reinforcement of calcium phosphate cement by incorporating with high-strength beta-tricalcium phosphate aggregates. J Biomed Mater Res B Appl Biomater 2012;100B(2):350–9.
[24] Puppi D, Chiellini F, Piras AM, Chiellini E. Polymeric materials for bone and cartilage repair. Prog Polym Sci 2010;35(4):403–40.
[25] Rodenas-Rochina J, Ribelles JL, Lebourg M. Comparative study of PCL-HAp and PCL-bioglass composite scaffolds for bone tissue engineering. J Mater Sci Mater Med 2013;24(5):1293–308.
[26] Hutmacher DW, Woodruff MA. The return of a forgotten polymer-polycaprolactone in the 21st century. Prog Polym Sci 2010;35(10):1217–56.
[27] Krupa I, Cecen V, Boudenne A, Prokeš J, Novák I. The mechanical and adhesive properties of electrically and thermally conductive polymeric composites based on high density polyethylene filled with nickel powder. Mater Des 2013;51:620–8.
[28] Al-Abdullat Y, Tsutsumi S, Nakajima N, Ohta M, Kuwahara H, Ikeuchi K. Surface modification of magnesium by NaHCO(3) and corrosion behavior in Hank's solution for new biomaterial applications. Mater Trans 2001;42(8):1777–80.
[29] Witte F. The history of biodegradable magnesium implants: a review. Acta Biomater 2010;6(5):1680–92.
[30] Song G. Control of biodegradation of biocompatable magnesium alloys. Corros Sci 2007;49(4):1696–701.
[31] Boccaccini AR, Hoppe A, Guldal NS. A review of the biological response to ionic dissolution products from bioactive glasses and glass-ceramics. Biomaterials 2011;32(11):2757–74.
[32] Dhert WJA, van Gaalen SM, Kruyt MC, Geuze RE, de Bruijn JD, Alblas J. Use of fluorochrome labels in in vivo bone tissue engineering research. Tissue Eng Part B Rev 2010;16(2):209–17.
[33] Habibovic P, Kruyt MC, Juhl MV, Clyens S, Martinetti R, Dolcini L, et al. Comparative in vivo study of six hydroxyapatite-based bone graft substitutes. J Orthop Res 2008;26(10):1363–70.
[34] Rahn BA, Perren SM. Xylenol orange, a fluorochrome useful in polychrome sequential labeling of calcifying tissues. Stain Technol 1971;46(3):125–9.
[35] Peake BM, Ashoka S, Bremner G, Hageman KJ, Reid MR. Comparison of digestion methods for ICP-MS determination of trace elements in fish tissues. Anal Chim Acta 2009;653(2):191–9.
[36] Cubadda F, Raggi A, Coni E. Element fingerprinting of marine organisms by dynamic reaction cell inductively coupled plasma mass spectrometry. Anal Bioanal Chem 2006;384(4):887–96.
[37] Erben RG. Embedding of bone samples in methylmethacrylate: an improved method suitable for bone histomorphometry, histochemistry, and immunohistochemistry. J Histochem Cytochem 1997;45(2):307–13.
[38] Banse X, Sims TJ, Bailey AJ. Mechanical properties of adult vertebral cancellous bone: correlation with collagen intermolecular cross-links. J Bone Miner Res 2002;17(9):1621–8.
[39] Zreiqat H, Howlett CR, Zannettino A, Evans P, Tanzil GS, Knabe C, et al. Mechanisms of magnesium-stimulated adhesion of osteoblastic cells to commonly used orthopaedic implants. J Biomed Mater Res 2002;62(2):175–84.
[40] Li L, Gao J, Wang Y. Evaluation of cyto-toxicity and corrosion behavior of alkali-heat-treated magnesium in simulated body fluid. Surf Coat Technol 2004;185(1):92–8.
[41] Rude RK, Gruber HE, Norton HJ, Wei LY, Frausto A, Mills BG. Bone loss induced by dietary magnesium reduction to 10% of the nutrient requirement in rats is associated with increased release of substance P and tumor necrosis factor-alpha. J Nutr 2004;134(1):79–85.
[42] Rude RK, Gruber HE, Norton HJ, Wei LY, Frausto A, Kilburn J. Dietary magnesium reduction to 25% of nutrient requirement disrupts bone and mineral metabolism in the rat. Bone 2005;37(2):211–9.
[43] Toba Y, Kajita Y, Masuyama R, Takada Y, Suzuki K, Aoe S. Dietary magnesium supplementation affects bone metabolism and dynamic strength of bone in ovariectomized rats. J Nutr 2000;130(2):216–20.
[44] Matinlinna JP, Areva S, Lassila LVJ, Vallittu PK. Characterization of siloxane films on titanium substrate derived from these aminosilanes. Surf Interface Anal 2004;36:1314–22.
[45] Sabzi M, Mirabedini SM, Zohuriaan-Mehr J, Atai M. Surface modification of TiO_2 nano-particles with silane coupling agent and investigation of its effect on the properties of polyurethane composite coating. Prog Org Coat 2009;65:222–8.
[46] Lin J, Siddiqui JA, Ottenbrite RM. Surface modification of inorganic oxide particles with silane coupling agent and organic dyes. Polym Adv Technol 2001;12(5):285–92.
[47] Wang TX, Chow LC, Frukhtbeyn SA, Ting AH, Dong QX, Yang MS, et al. Improve the strength of PLA/HA composite through the use of surface initiated

polymerization and phosphonic acid coupling agent. J Res Natl Inst Stand Technol 2011;116(5):785–96.
[48] Shen YH, Liu WC, Lin KL, Pan HB, Darvell BW, Peng SL, et al. Interfacial pH: a critical factor for osteoporotic bone regeneration. Langmuir 2011;27(6): 2701–8.
[49] Kuwahara H, Al-Abdullat Y, Mazaki N, Tsutsumi S, Aizawa T. Precipitation of magnesium apatite on pure magnesium surface during immersing in Hank's solution. Mater Trans 2001;42(7):1317–21.
[50] Zhang EL, Yang L. Biocorrosion behavior of magnesium alloy in different simulated fluids for biomedical application. Mat Sci Eng C-Bio S 2009;29(5): 1691–6.
[51] Zhang EL, Xu LP, Yu GN, Pan F, Yang K. In vivo evaluation of biodegradable magnesium alloy bone implant in the first 6 months implantation. J Biomed Mater Res A 2009;90A(3):882–93.
[52] Dupraz AMP, vandenMeer SAT, DeWijn JR, Goedemoed JH. Biocompatibility screening of silane-treated hydroxyapatite powders, for use as filler in resorbable composites. J Mater Sci Mater Med 1996;7(12):731–8.
[53] Hussain A, Bessho K, Takahashi K, Tabata Y. Magnesium calcium phosphate as a novel component enhances mechanical/physical properties of gelatin scaffold and osteogenic differentiation of bone marrow mesenchymal stem cells. Tissue Eng Part A 2012;18(7–8):768–74.
[54] Witte F, Kaese V, Haferkamp H, Switzer E, Meyer-Lindenberg A, Wirth CJ, et al. In vivo corrosion of four magnesium alloys and the associated bone response. Biomaterials 2005;26(17):3557–63.
[55] Li Z, Gu X, Lou S, Zheng Y. The development of binary Mg-Ca alloys for use as biodegradable materials within bone. Biomaterials 2008;29(10):1329–44.
[56] Vormann J. Magnesium: nutrition and metabolism. Mol Aspects Med 2003;24:27–37.
[57] Xu L, Yu G, Zhang E, Pan F, Yang K. In vivo corrosion behavior of Mg-Mn-Zn alloy for bone implant application. J Biomed Mater Res A 2007;83A(3):703–11.
[58] Berlemann U, Ferguson SJ, Nolte LP, Heini PF. Adjacent vertebral failure after vertebroplasty. J Bone Joint Surg Br 2002;84:748–52.
[59] Frankel BM, Monroe T, Wang C. Percutaneous vertebral augmentation: an elevation in adjacent-level fracture risk in kyphoplasty as compared with vertebroplasty. Spine J 2007;7:575–82.